Spike pattern detection with close-to-biology spiking neuronal network

Takuya Nanami
Institute of Industrial Science, The University of Tokyo, Tokyo, Japan.

Takashi Kohno
Institute of Industrial Science, The University of Tokyo, Tokyo, Japan.

E-mail: nanami@iis.u-tokyo.ac.jp, kohno@g.ecc.u-tokyo.ac.jp

Abstract

The nervous system contains a variety of neuron types, each with different electrophysiological properties. However, their roles in information processing are poorly understood. Using the piecewise quadratic neuron (PQN) model that can reproduce a variety of electrophysiological properties, we demonstrate that performance on a biologically plausible task of spike pattern detection varies depending on the electrophysiological properties.

Keywords: Spiking neural network, Pattern detection, PQN model

1. Introduction

In the nervous system, neurons exhibit a variety of electrophysiological properties. For example, when given a gradually increasing stimulus input, Class I neurons in the Hodgkin's classification [1] start firing at a frequency close to zero, whereas Class II neurons start firing at a certain higher frequency. In addition, when given a step current input, neurons in the regular spiking class exhibit spike-frequency adaptation, in which the firing frequency gradually decreases, whereas neurons in the fast spiking class fire at an almost constant frequency. Furthermore, bursting neuron classes such as elliptic bursting and parabolic bursting are known to alternate between intense firing and resting state in response to constant stimuli. The mathematical structures behind these diverse electrophysiological properties of neurons have been intensively investigated, and spiking neuron models that reproduce them have also been developed [2][3][4][5][6][7][8][9][10][11][12][13]. However, the role of these electrophysiological properties of neurons in information processing in the nervous system remains unclear. This is because the information processing mechanisms in the brain microcircuits are too complex and poorly understood to assess the contribution of each electrophysiological properties. In addition, there are various technical hurdles in measuring neuronal activities in vivo, which also make it difficult to analyze the role of electrophysiological properties.

In this study, we investigate the relationship between the electrophysiological properties of neurons and the learning properties of a network using in silico simulations. We employ simple and biologically plausible network structure and task proposed in the previous studies [14][15]. For the spiking neuron model, we adopt the piecewise quadratic neuron (PQN) model [13], which is a lightweight model that can reproduce a wide variety of electrophysiological properties. Although there are a variety of dynamics behind the neuronal activities, here we focus on the most fundamental dynamics, the spike generation. We investigate how the success rate of pattern detection changes while varying the mathematical structure of the fast subsystem responsible for the spike generation. We show how the success rate depends on the dynamical structure in the fast subsystem.

The remainder of this paper is organized as follows: Section 2 describes the details of the methods, Section 3 shows the simulation results, and Section 4 summarizes the work and suggests ideas for future.

2. Methods

2.1. *Network model*

The network structure, input data, and learning rule, which we briefly describe in this section, are largely the same as those proposed in the previous study [15]. The differences are in the neuron and synapse models, the number of input nodes (reduced from 2000 to 512), and the number of patterns to be detected. Figure 1 shows the network architecture comprising input nodes, output neurons, and excitatory and inhibitory synapses. 512 input nodes transmit spike trains to 9 output neurons through excitatory synapses, whose synaptic efficacies are updated based on the spike timing-dependent plasticity (STDP) rule. The output neurons are the PQN model. They are connected by the inhibitory synapses each other, whose synaptic efficacies are fixed. A stimulus input to the j-th neuron is written as follows:

$$I_{j_k} = p_0 \sum_{i=1}^{512} w_{ji}^{e} x_i - p_1 \sum_{i=1(i \neq j)}^{9} w_{ji}^{i} s_i \qquad (1)$$

where x_i represents the activation of the i-th input node, which is 0 or 1. s_i is an inhibitory synaptic current from the i-th neuron. w_{ji}^{e} is the efficacy of the excitatory synapse from the i-th node to j-th neuron. w_{ji}^{i} is the efficacy of the inhibitory synapse from the i-th neuron to j-th neuron. Parameters p_0 and p_1 control the amount of excitatory and inhibitory stimulus.

Figure 2 shows an example of the input data. Three different spike patterns (colored dots) are embedded in random spikes (black dots). These spike trains are generated based on the Poisson process. First, an 80-second training period is given to learn excitatory synapses based on the STDP. Then, a 20-second test period is given to assess whether the output neurons are firing in response to the spike patterns. The task is considered successful when all spike patterns are detected by at least one output neuron with a probability of 90% or greater during the test period.

The rule for updating the synaptic efficacy based on the STDP is given by

$$\Delta w_{ji}^{e} = \begin{cases} a^{+} \exp\left(\dfrac{t_i - t_j}{\tau^{+}}\right) & \text{if } t_i \leq t_j, \\ a^{-} \exp\left(-\dfrac{t_i - t_j}{\tau^{-}}\right) & \text{if } t_i > t_j. \end{cases} \qquad (1)$$

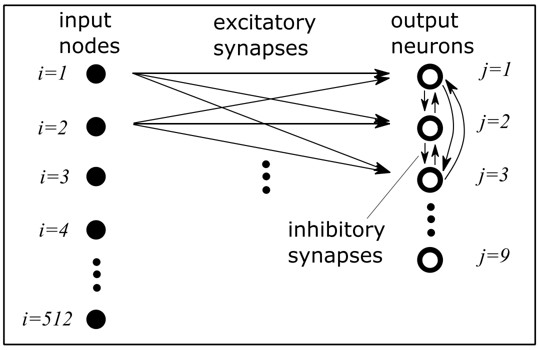

Figure 1. Network architecture.

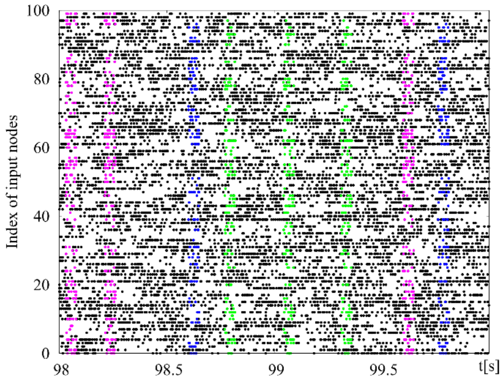

Figure 2. Input data.

where t_j is the spike timing of the presynaptic node and t_j is the spike timing of the postsynaptic neuron. τ^{+} and τ^{-} control the time constant of the long-term potentiation and depression, respectively. a^{+} and a^{-} determine the learning rate.

2.2. *Neuron model*

The PQN model is a qualitative spiking neuron model that supports a wide variety of spiking properties with a limited computational cost. The equations for the PQN model in two-variable mode are as follows:

$$\frac{dv}{dt} = \frac{\emptyset}{\tau}(f(v) - n + I_0 + kI_{stim}), \qquad (1)$$

$$\frac{dn}{dt} = \frac{1}{\tau}(g(v) - n), \qquad (2)$$

$$f(v) = \begin{cases} a_{fn}(v - b_{fn})^2 + c_{fn} & (v < 0) \\ a_{fp}(v - b_{fp})^2 + c_{fp} & (v \geq 0), \end{cases} \qquad (3)$$

$$g(v) = \begin{cases} a_{gn}(v - b_{gn})^2 + c_{gn} & (v < r_g) \\ a_{gp}(v - b_{gp})^2 + c_{gp} & (v \geq r_g), \end{cases} \qquad (4)$$

where v and n correspond to the membrane potential and recovery variable, respectively. Parameter I_0 is a bias constant. I_{stim} is the stimulus input and k is its scaling parameter. The parameters τ and $\emptyset$ determine the time constants of the variables. The parameters r_g, a_x, b_x, and c_x, where x is fn, fp, gn, or gp, are constants that determine the nullclines of the variables. Constants b_{fp}, c_{fp}, b_{gp}, and c_{gp}, are determined by other parameters such that the nullclines are continuous and smooth (see [13]). All of the variables and parameters are purely abstract with no physical units.

We prepared parameter sets, each with different dynamics of the spike generation, by varying the two key parameters, a_{gn} and $\emptyset$. The parameter a_{gn} determines the slope of the left portion of the *n*-nullcline. For example, if the a_{gn} is reduced from 0.75 to 0, the slope on the left portion of the *n*-nullcline decreases and the position of the bifurcation point shifts to the right (Fig. 3 (A-B)). The parameter $\emptyset$ controls the time constant of *v* and affects the trajectory of the stable limit cycle. If the $\emptyset$ increases from 0.35 to 1, the trajectory is extended especially in the negative direction of the *v*-axis (Fig. 3 (B-C)). We prepared twelve parameter sets consisting of the combination of four different values of a_{gn} (1.75, 0.75, 0.25, and 0) and three different values of $\emptyset$ (0.35, 0.5, and 1).

3. Results

Figure 4 shows the success rate for each parameter set. We varied the number of patterns from 1 to 5 and measured the average success rate. We performed 128 trials for each number of patterns, resulting in a total of 640 trials. For fair comparison, parameters, I_0, τ, p_0, and p_1 were chosen to achieve the best success rate. First, the values of these parameters were determined randomly, and then these parameters were iteratively updated by the differential evolution (DE) algorithm [16] while evaluating the success rate. We used 64 individuals and 200 generations for the DE algorithm. The results show that as the a_{gn} becomes smaller and $\emptyset$ becomes larger, a higher success rate tends to be obtained.

4. Conclusion

In this study, we prepared twelve types of dynamical structures in the neurons and investigated how the differences in their dynamics affect performance in a biologically plausible task. The results showed that better performance was obtained when the a_{gn} is small and $\emptyset$ is large. As the a_{gn} becomes smaller, the bifurcation

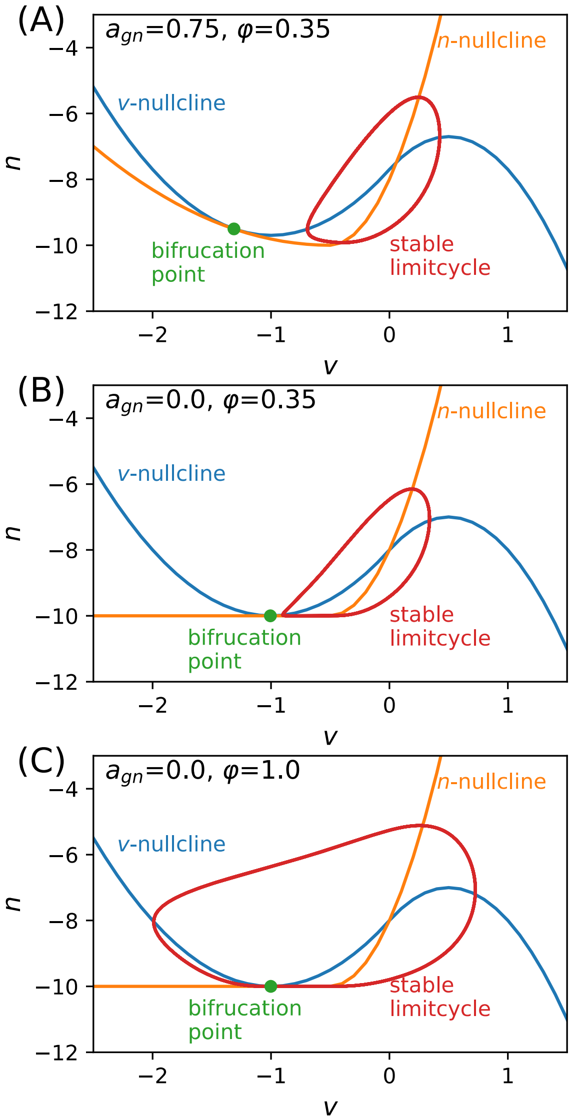

Figure 3. Mathematical structure.

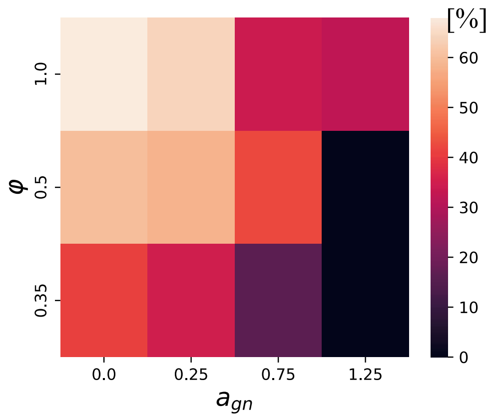

Figure 4. Success rate.

point approaches $v = 0$. Note that $v = 0$ is supposed to be the point of transmitter release in the PQN network. When the bifurcation point is close to this point, neurons require less time to fire. Considering the exponential decay of the STDP curve, such neurons can obtain a larger Δw than those fire more slowly. It may cause the higher success rate.

As the $\emptyset$ increases, the stable limit cycle is extended in the negative direction of the v-axis. Consequently, the trajectory goes through a narrow channel and takes a long time to generate the second spike. Considering that inputs of sufficient magnitude are usually instantaneous, such neurons will rarely generate a second spike. Since the second spike may cause pairing with spike signals unrelated to the target pattern, the neurons with a larger $\emptyset$ will stably detect patterns by avoiding the second spike.

In our future work, we will verify these hypotheses and investigate the impact of other neuronal dynamics, such as spike frequency adaptation and bursting, on the success rate of the task.

Acknowledgment

This study was partially supported by JSPS KAKENHI Grant Number 21K17849.

References

1. A. L. Hodgkin, "The local electric changes associated with repetitive action in a non-medullated axon." The Journal of physiology, vol. 107, no. 2, pp. 165–181, Mar. 1948.
2. X.-J. Wang, "Ionic basis for intrinsic 40 hz neuronal oscillations", NeuroReport, vol. 5, pp. 221–224, 1993.
3. R. E. Plant, "Bifurcation and resonance in a model for bursting nerve cells", Journal of Mathematical Biology, vol. 67, pp. 15–32, 1981.
4. J. Rinzel and B. Ermentrout, "Analysis of neural excitability and oscillations", in Methods in Neuronal Mod- eling, Second Edition, C. Koch and I. Segev, Eds. MIT Press, 1998, ch. 7, pp. 251–292.
5. E. M. Izhikevich, "Simple model of spiking neurons", IEEE Trans. Neural Networks, pp. 1569–1572, 2003.
6. R. Brette and W. Gerstner, "Adaptive Exponential Integrate-and-Fire Model as an Effective Description of Neuronal Activity", J. Neurophysiol., vol. 94, pp. 3637–3642, 2005.
7. E. Izhikevich, "Dynamical systems in neuroscience", MIT Press, p. 111, Jul. 2007.
8. M. Pospischil, M. Toledo-Rodriguez, C. Monier, Z. Piwkowska, T. Bal, Y. Fregnac, H. Markram, and A. Destexhe, "Minimal hodgkin-huxley type models for different classes of cortical and thalamic neurons", Biological Cybernetics, vol. 99, no. 4-5, pp. 427–441, 2008.
9. T. Nanami and T. Kohno, "Simple cortical and thalamic neuron models for digital arithmetic circuit implementation", Frontiers in Neuroscience, section Neuromorphic Engineering, vol. 10, no. 181, 2016.
10. T. Nanami, K. Aihara, and T. Kohno, "Elliptic and parabolic bursting in a digital silicon neuron model", in 2016 International Symposium on Nonlinear Theory and Its Applications, November 2016, pp. 198–201.
11. T. Nanami, F. Grassia, and T. Kohno, "A parameter optimization method for digital spiking silicon neuron model", Journal of Robotics Networking and Artificial Life, vol. 4, no. 1, pp. 97–101, 2017.
12. T. Nanami, F. Grassia, and T. Kohno, "A metaheuristic approach for parameter fitting in digital spiking silicon neuron model", Journal of Robotics Networking and Artificial Life, vol. 5, no. 1, pp. 32–36, 2018.
13. T. Nanami and T. Kohno, "Piecewise Quadratic Neuron model : a tool for close-to-biology spiking neuronal network simulation on dedicated hardware", Frontiers in Neuroscience, section Neuromorphic Engineering, in press.
14. T. Masquelier, R. Guyonneau, and S. J. Thorpe, "Spike timing dependent plasticity finds the start of repeating patterns in continuous spike trains", PLOS ONE, vol. 3, pp. 1–9, 01 2008.
15. T. Masquelier, R. Guyonneau, and S. J. Thorpe, "Competitive STDP-Based Spike Pattern Learning", Neural Computation, vol. 21, no. 5, pp. 1259–1276, 05 2009.
16. R. Storn and K. Price, "A simple and efficient heuristic for global optimization over continuous spaces", Journal of Global Optimization, vol. 11, no. 4, pp. 341–359, 1997.

Authors Introduction

Dr. Takuya Nanami

He received the Ph.D from University of Tokyo in 2019. He is a research associate in Institute of Industrial Science, University of Tokyo since 2020.

Prof. Takashi Kohno

He received the B.E. degree in medicine (1996) and the Ph.D. degree in mathematical engineering (2002) from University of Tokyo, Japan. He is a professor in Institute of Industrial Science, University of Tokyo since 2018.